JOURNAL OF MATERIALS SCIENCE **35** (2000) 123–126

Electrical conductivity of molybdenum phosphate ($MoO_3 : P_2O_5$) glasses

A. M. AL-SHUKRI *, G. D. KHATTAK, M. A. SALIM
Department of Physics, King Fahd University of Petroleum and Minerals,
Dhahran 31261, Saudi Arabia
E-mail: alshukri@kfupm.edu.sa

The dc conductivity of molybdenum phosphate glasses with the batch composition $[(MoO_3)_z(P_2O_5)_{z-1}]$ where $z = 0.55$, 0.60, 0.65, 0.70, and 0.75 has been studied. The non-linearity of the Arrhenius plot ($\ln(\sigma)$ versus T^{-1}) may be due to processes involving several similar activation energies, conduction by small polarons, or variable range hopping of carriers. The electrical conductivity results for these glasses have been discussed by applying the two models suggested by Meunier *et al.* and it has been found that the use of the small polaron model yields physically plausible values for W_H and W_D within experimental error. © *2000 Kluwer Academic Publishers*

1. Introduction

The 3d transition-metal (TM) oxide phosphate glasses have received considerable attention because of their semiconducting properties and potential applications [1–4]. The electrical conduction in the glasses occurs by electron hopping from an ion of the low valence state transition metal to an ion of the higher valence state. However, mathematical formulation of this process is difficult due to numerous material factors including the type and concentration of the TM ion, the number of valence states in which it can exist, the glass preparation conditions, and the possible existence of microscopic structures within the glass matrix.

The molybdenum phosphate ($MoO_3 : P_2O_5$) glass system represents a rather unique system in that it forms stable glasses over a wide and continuous composition range extending to about 86 mol % MoO_3 [5]. Moreover, since unmodified Mo-phosphate glasses are semiconducting [6] and can be chemically intercalated with Li_2O and Ag_2O [7], these glasses have technological potential in electrochemical applications. In electrochemical devices such as solid state batteries, these glasses could be used as both electrolyte and cathode materials. Since the cathode and electrolyte are formed from the same glass former, a common glassy network should result which would provide a continuum for the diffusion of the cations. This continuum should in principle eliminate the problem of interfacial chemical reactions and may minimize any over-potentials [8].

While small polaron theory has been extensively used to describe the electrical properties of a wide range of TM-oxide glasses [9–11], the best agreement between experiment and theory has been found for vanadate glasses such as V_2O_5-P_2O_5. It appears probable that the electrical properties of all the 3d transition-metal oxide phosphate glasses will not succumb to a single theory.

The experimental determination of activation energies from the electrical conductivity, σ, as a function of temperature, T, is sometimes different; the Arrhenius plot ($\ln(\sigma)$ versus T^{-1}) may not be linear. This may be due to process involving several similar activation energies, conduction by polarons [12–14] or variable range hopping of carriers [12, 15]. In this paper we discuss the electrical conductivity results for Mo-phosphate glasses by applying the two models suggested by Meunier *et al*. [16].

2. Experimental procedures

2.1. Glass preparation

The Mo-phosphate glasses were prepared by melting dry mixtures of reagent grade MoO_3 and P_2O_5 in alumina crucibles with the batch composition $[(MoO_3)_z(P_2O_5)_{1-z}]$ where $z = 0.55$, 0.60, 0.65, 0.70, and 0.75. Since the oxidation and reduction reactions in a glass melt are known to depend on the size of the melt, the sample geometry, whether the melt is static or stirred, thermal history and quenching rate, all glass samples were prepared under similar conditions to minimize these factors. Approximately 40 g of chemicals were thoroughly mixed to obtain homogenized batches. The crucible containing the batch mixture was placed in the furnace, heated at 300 °C for an hour in order to minimize volatilization, and subsequently transferred to a melting furnace maintained at a temperature of 1200 °C. The melt was left for about 4 h under atmospheric conditions in the furnace during which the melt was occasionally stirred with alumina rod. The homogenized melt was then cast onto a stainless steel plate

---

* Author to whom all correspondence should be addressed.

0022–2461

TABLE I Batch and actual composition of various $(MoO_3)_z(P_2O_5)_{1-z}$ glasses

Sample (z)	Batch (z)	Actual (from ICP) (z)	Actual (from ICP) ($1-z$)
G55	0.55	0.65	0.35
G60	0.60	0.70	0.30
G65	0.65	0.68	0.32
G70	0.70	0.65	0.35
G75	0.75	0.74	0.26

mold to form glass buttons. The batch and actual compositions of the various Mo-phosphate glasses studied are listed in Table I with the actual compositions determined by inductively coupled plasma spectroscopy (ICP). Even though a uniform spread in batch Mo compositions was attempted, the resulting glasses formed essentially at four Mo values: 0.65, 0.68, 0.70, and 0.74. It is expected that the actual compositions of these glasses might vary from the batch compositions due to the loss of oxygen as Mo^{6+} ions are reduced to Mo^{5+} and to different vaporization rates of MoO_3 and P_2O_5 during the melting process. Generally the reduction of Mo^{6+} has been found to be small in previous investigations [5, 17], thus the variation in the vaporization rates is the more probable source for the deviation from the batch compositions.

2.2. dc conductivity measurements

For dc conductivity measurements disc-shaped samples were made. The samples were polished and then the evaporation of gold electrodes on polished surfaces was carried out in vacuum. Measurement of dc conductivity as a function of temperature, in all the samples, was made by two probe technique. The current in the samples was measured using a Keithley 485 auto ranging pico ammeter. To obtain the variation of resistivity with temperature, the sample was placed in a furnace, brought to the desired temperature and maintained at that temperature for sufficient time before taking the measurements to ensure thermal stability. The temperature was measured by a Pt/Pt-10% Rh thermocouple.

3. Results and discussion

A general expression for dc electrical conductivity, σ, in semiconductors and in insulators is

$$\sigma(T) = A(T)\exp[-\beta W(T)], \tag{1}$$

where T is the temperature, $\beta^{-1} = k_B T$, k_B is the Boltzmann constant, and $A(T)$ and $W(T)$ are assumed to be slowly varying functions of the temperature. The usual analysis of the conduction curve by Arrhenius plot calculates the slope, or $W'(T)/k_B$ where

$$W'(T) = -\frac{\partial \ln(\sigma)}{\partial \beta} = k_B T^2 \frac{\partial \ln(\sigma)}{\partial T} \tag{2}$$

$$W'(T) = W(T) - \frac{\partial \ln[A(T)]}{\partial \beta} + \beta \frac{\partial W(T)}{\partial \beta} \tag{3}$$

TABLE II A and average activation energy for various $(MoO_3)_z(P_2O_5)_{1-z}$ glasses

Sample (z)	$A(1/\Omega\cdot\mathrm{m})$	W(eV)
G55	0.22	0.52
G60	0.26	0.50
G65	0.53	0.54
G70	0.32	0.48
G75	1.04	0.50

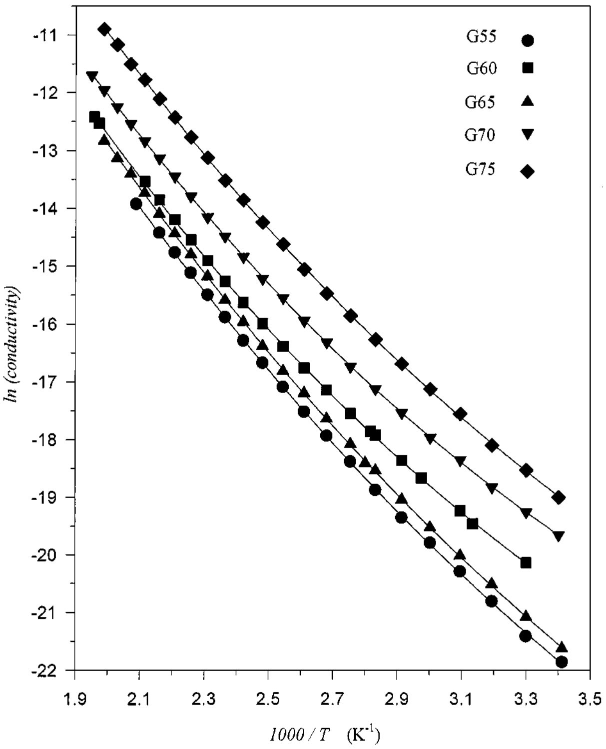

Figure 1 A plot of ln(σ) versus $1000/T$ for various $(MoO_3)_z(P_2O_5)_{1-z}$ glasses.

If there is reason to believe that A and W are temperature independent, then the slope should be constant, yielding directly the activation energy, W. So normally one could find the activation energy by plotting ln(σ) versus $1/T$ (Kelvin). From a straight line fit, the slope would give the activation energy W, assuming W independent of temperature. One can find A and the average activation energy for the given temperature range by fitting the data to a straight line. Results are shown in Table II. Fig. 1 shows the results of conductivity, σ, as a function of temperature, T, as plots of ln(σ) versus $1000/T$ for all the five samples which suggest that the plots are not strictly linear. Thus we follow the approaches suggested by Meunier *et al.* [16]. Because of the possible temperature dependence in W, Meunier *et al.* [16] suggests plots of W versus different variables depending upon the two models suggested.

i) For the **variable range hopping model**, an Arrhenius analysis Equation 3 yields the function

$$W'(T) = Bk_B\left(\frac{p+1}{p+4}\right)T^{3/(p+4)} \tag{4}$$

The constants B and p may be independently determined by finding the intercept and the slope,

TABLE III The values of p, B, $W'(\approx 300\text{ K})$ and $\Delta E(\approx 300\text{ K})$, θ_D, W_D, W_H and $2^{p/(p+4)}k_BT$ of various $(MoO_3)_z(P_2O_5)_{1-z}$ glasses

Sample	p	B	$W'(\approx 300$ K) (eV)	$\Delta E(\approx 300$ K) (eV)	θ_D (K)	W_D (eV)	W_H (eV)	$2^{p/(p+4)}k_BT$ (eV)
G55	−0.73	323	0.42	0.49	833	−0.65	1.15	0.022
G60	−1.20	−141	0.44	0.58	985	−0.55	1.14	0.021
G65	−1.06	−789	0.44	0.56	838	−0.60	1.14	0.020
G70	−1.23	−103	0.35	0.47	934	−0.65	1.15	0.019
G75	−1.05	−780	0.38	0.48	879	−0.72	1.19	0.020

respectively, on a $\ln W'$ versus $\ln T$ plot, where the slope $= 3/(p+4)$ and the y-intercept $= \ln[Bk_B(p+1)/(p+4)]$. The function $W'(T)$ also gives the hopping energy through the relation [18]

$$\Delta E = 2^{-p/(p+4)}W' \tag{5}$$

This energy varies continuously from W' to $W'/2$ as p increases from 0 to a large value. Finally, as a check on the validity of this model, according to Mott [12, 15] the energy W' must satisfy

$$W'(T) < 2^{p/(p+4)}k_BT \tag{6}$$

Fig. 2 shows a plot of $\ln W'$ versus $\ln T$ for a representative sample, G55. The values of p, B, $W'(\approx 300\text{ K})$ and $\Delta E(\approx 300\text{ K})$ obtained for all the samples are given in Table III. We see (Table III) that Condition 6 is not satisfied and so the variable range hopping model cannot be applied here.

ii) **Conduction by small polarons**: Schnakenberg [19] has analyzed the non-adiabatic hopping energy W of small polarons at temperatures above $\theta_D/4$, where θ_D is the Debye temperature of the optical phonons of the solid, and he deduced the following high temperature relation:

$$W(T) = W_H\left(\frac{\tanh(\theta_D/4T)}{(\theta_D/4T)}\right) + \frac{W_D}{2} \tag{7}$$

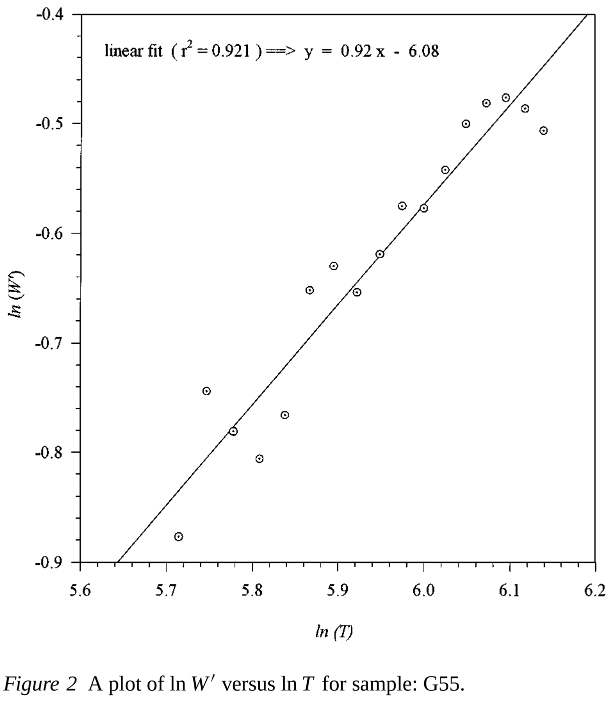

Figure 2 A plot of $\ln W'$ versus $\ln T$ for sample: G55.

where W_D and W_H are two constants (disorder energy and high temperature small polaron hopping energy, respectively). Moreover, the conductivity $\sigma(T)$ is given by Equation 1, with the above expression for $W(T)$ and a prefactor, A, which is constant or depends only very weakly on temperature. Fitting the constants of the model using an Arrhenius plot analysis, this involves the energy

$$W'(T) = W_H\,\mathrm{sech}^2(\theta_D/4T) + \frac{W_D}{2} \tag{8}$$

The parameters W_H, W_D, and θ_D are determined in a two step process. First we assume $W_D = 0$ and expanding $\mathrm{sech}^2(x)$ function into power series $1 - x^2 + \cdots$, Equation 8 becomes

$$W'(T) = W_H\{1 - (\theta_D/4T)^2 + \cdots\} \tag{9}$$

A plot of W' versus T^{-2} should yield a straight line at the higher temperatures, from which the intercept is W_H and the slope $= W_H(\theta_D/4T)^2$. The data is then replotted as W' versus $\mathrm{sech}^2(\theta_D/4T)$ using θ_D value determined in the preceding plot. A straight line should yield the intercept $= W_D/2$ and slope $= W_H$. Fig. 3 show

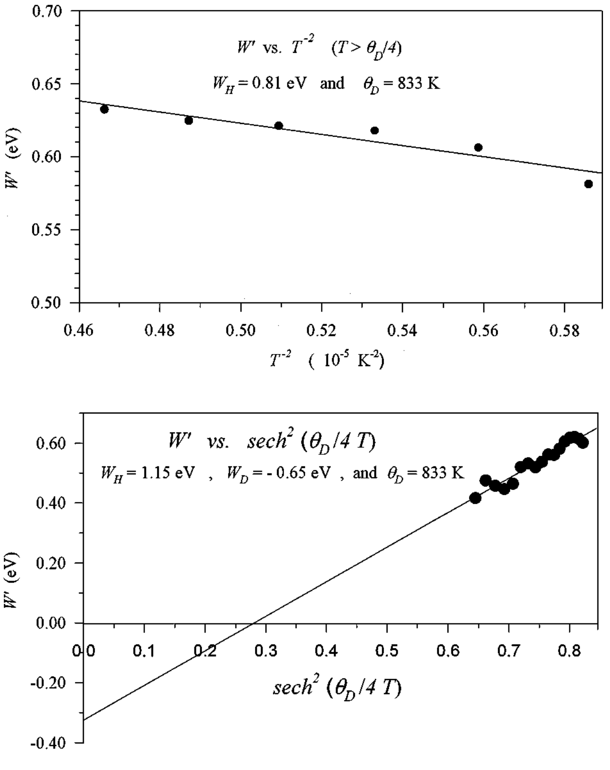

Figure 3 Plots of W' versus T^{-2} and W' versus $\mathrm{sech}^2(\theta_D/4T)$ for sample: G55.

plots of W' versus T^{-2} and W' versus $\mathrm{sech}^2(\theta_D/4T)$. The values of θ_D, W_D, and W_H determined are listed in Table III.

We see [Table III] that use of the small polaron model to calculate $W'(T)$ yields physically plausible values for W_H and W_D within experimental error. The values of the Debye temperature θ_D are a factor of up to 3 too large compared to θ_D obtained from ultrasonic investigation [17]. However, the values obtained here can not be compared with those given in [17]. The Debye temperature reported here in this work is that of the optical phonons, however the Debye temperature determined by Patel and Bridges [17] is that of the acoustic phonons, the one determined from heat capacity and ultrasonic measurements. That is to say, that the Debye temperature in the small polaron model is associated with the frequency of the optical phonons, while the Debye temperature determined from the ultrasonic data of Patel and Bridge [17] for the Mo-phosphate glasses is associated with the acoustic phonons and no correlation between the frequency of these two types of phonons has been reported in the literature.

Acknowledgements

The support of KFUPM Physics Department is acknowledged.

References

1. J. D. MACKENZIE, in "Modern Aspects of the Vitreous State," Vol. 3 (Butterworth and Co., London, 1964).
2. N. F. MOTT, *J. Non-Crystalline Solids* **1** (1968) 1.
3. D. ADLER, in "Amorphous Semiconductors" (CRC Press, Cleveland, Ohio, 1971).
4. I. G. AUSTIN and E. J. GARBETT, in "Electronic and Structural Properties of Amorphous Semiconductors," edited by P. G. LeComber and J. Mart (Academic Press, London, 1973).
5. B. BRIDGE and N. D. PATEL, *J. Mater. Sci.* **21** (1986) 1187.
6. M. H. HEKMAT-SHOAR, C. A. HOGARTH and G. R. MORIDI, *ibid.* **20** (1985) 889.
7. B. V. R. CHOWDARI, K. L. TAN, W. T. CHIA and R. GOPALAKRISNAN, *J. Non-Crystalline Solids* **128** (1991) 18.
8. J. L. SOUQUET, *Solid State Ionics* **28–30** (1988) 693.
9. N. F. MOTT, *J. Non-Crystalline Solids* **1** (1968) 1.
10. M. SAYER and A. MANSINGH, *Phys. Rev.* **B6** (1972) 4629.
11. L. MURASKI, G. H. CHUNG and J. D. MACKENZIE, *J. Non-Crystalline Solids* **32** (1979) 208.
12. N. F. MOTT and E. A. DAVIS, "Electronic Processes in Non-Crystalline Materials," 2nd ed. (Clarendon, Oxford, 1979).
13. I. G. AUSTIN and N.F. MOTT, *Adv. Phys.* **18** (1969) 41.
14. T. HOLSTEIN, *Ann. Phys.* **8** (1959) 342.
15. N. F. MOTT, *Phil. Mag.* **19** (1969) 835.
16. M. MEUNIER, J. F. CURRIE, M. R. WERTHEIMER and A. YELON, *J. Non-Crystalline Solids* **46** (1981) 433.
17. N. D. PATEL and B. BRIDGE, *Phys. Chem. Glasses* **24** (1983) 130.
18. E. H. HAMILTON, *Phil. Mag.* **26** (1972) 1043.
19. J. SCHNAKENBERG, *Phys. Stat. Solidi* **28** (1968) 623.

Received 9 April 1998
and accepted 15 June 1999